Electronic Supplementary Material (ESI) for Inorganic Chemistry Frontiers.
This journal is © the Partner Organisations 2022

Supporting Information

Anomalous Thermal Expansion of Strontium Squarate Trihydrate Induced by Hydrogen-bond Weakening

Zhanning Liu,[a, c]* Zhe Wang,[b] Chengyong Xing,[a] Jian Tian[a] and Xianran Xing[d]

a. School of Materials Science and Engineering, Shandong University of Science and Technology, Qingdao, 266590, China.
b. School of Materials Science and Engineering, China University of Petroleum (East China), Qingdao, Shandong, 266580, China.
c. State Key Laboratory of Structural Chemistry, Fujian Institute of Research on the Structure of Matter, Chinese Academy of Sciences, Fuzhou, Fujian 350002, China.
d. Beijing Advanced Innovation Center for Materials Genome Engineering, Institute of Solid State Chemistry, University of Science and Technology Beijing, Beijing, 100083, China.

Contents

Figure S1 TG-DSC curve of Sr-sq.....3

Figure S2 *In situ* VT-PXRD patterns of Sr-sq upon heating under N_2.....3

Figure S3 Lebail fitting pattern of Sr-sq (at 300K), the fitting result is R_{wp} = 7.2%, R_p = 5%...4

Figure S4 Temperature dependent lattice constant changes of the monoclinic phase Sr-sq obtained from Lebail fitting.....5

Figure S5 Illustration of the relationship between principal axes (blue lines) and orthorhombic axes (black arrows).....5

Table S1 Crystallographic data of compound Sr-sq at different temperatures.....6

Table S2 Bond lengths of Sr-sq at different temperatures.....7

Table S3 Temperature dependent angle changes of φ_1 and φ_2.....7

Figure S6 Temperature dependent low frequency (below 200 cm^{-1}) Raman mode shifts. 8

Figure S7 Experimental measured (black) and DFT calculated (red) Raman spectrum of Sr-sq. 8

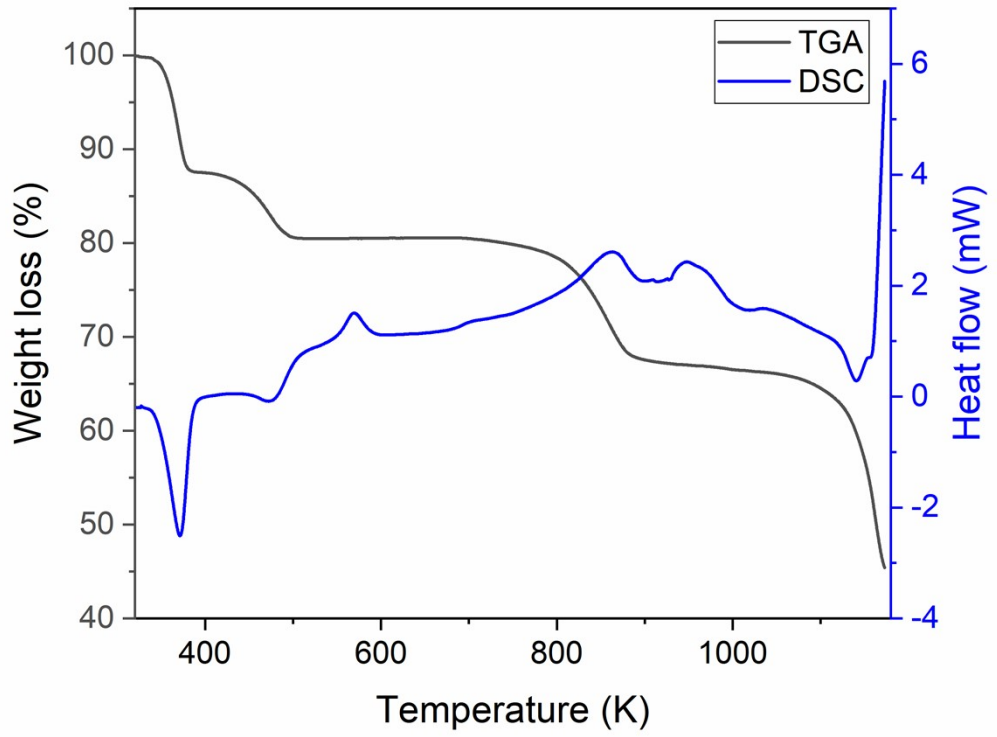

Figure S1 TG-DSC curve of **Sr-sq.**

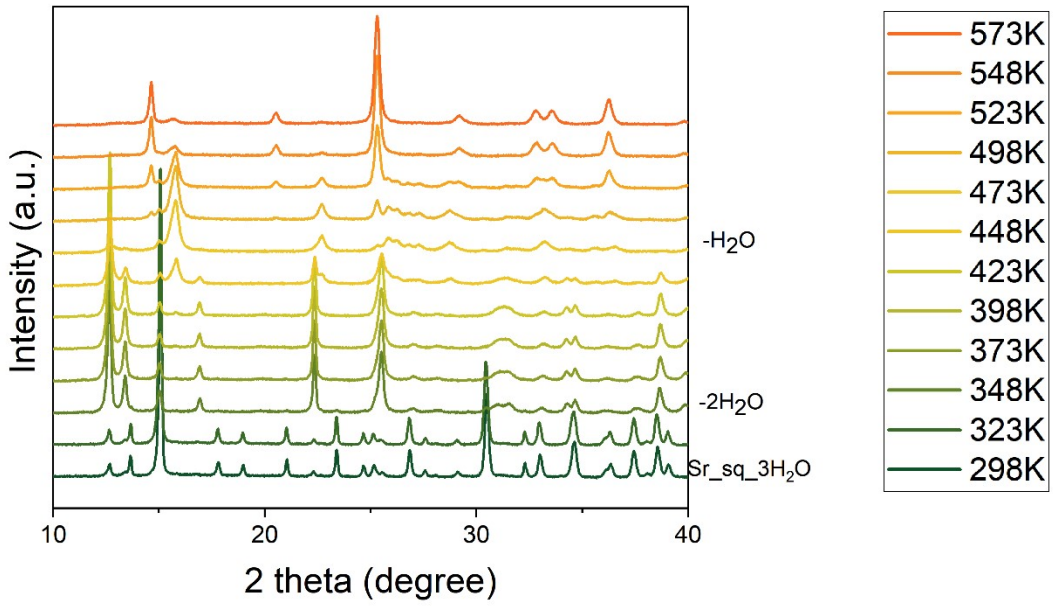

Figure S2 *In situ* VT-PXRD patterns of **Sr-sq** upon heating under N_2.

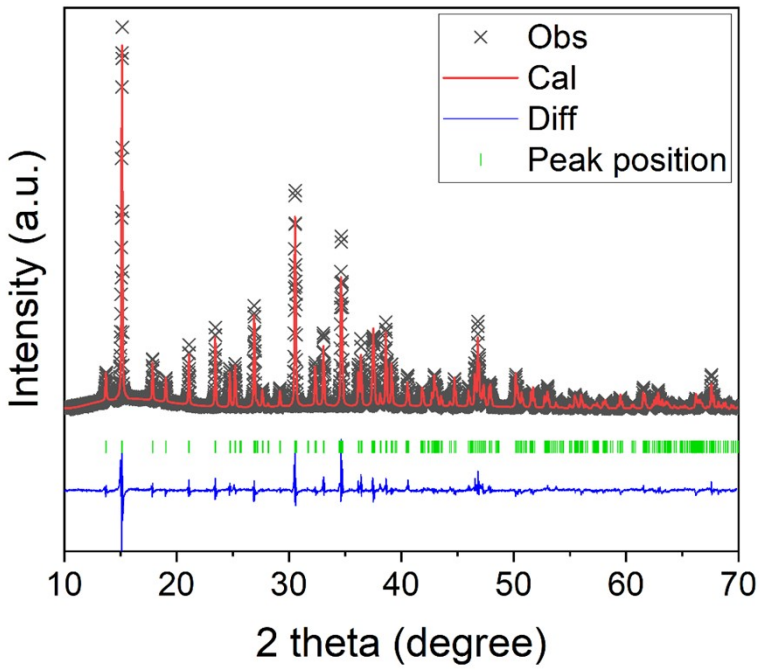

Figure S3 Lebail fitting pattern of **Sr-sq** (at 300K), the fitting result is R_{wp} = 7.2%, R_p = 5%.

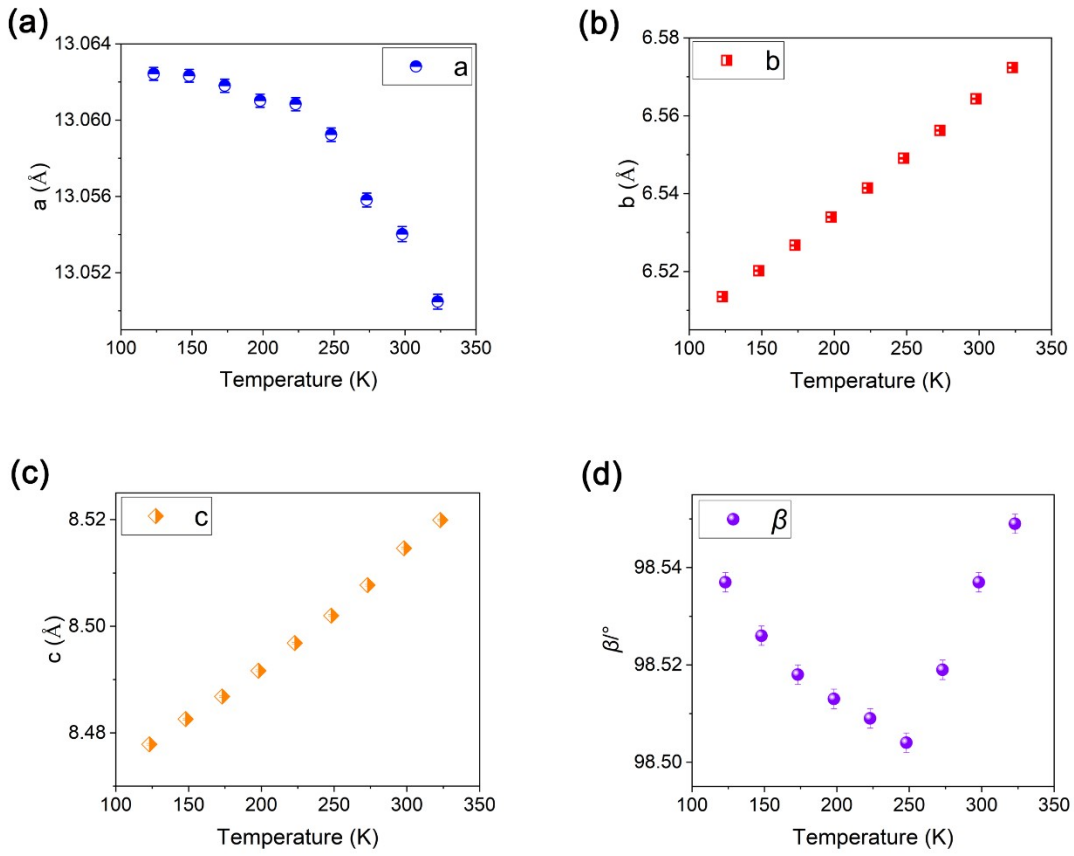

Figure S4 Temperature dependent lattice constant changes of the monoclinic phase **Sr-sq** obtained from Lebail fitting.

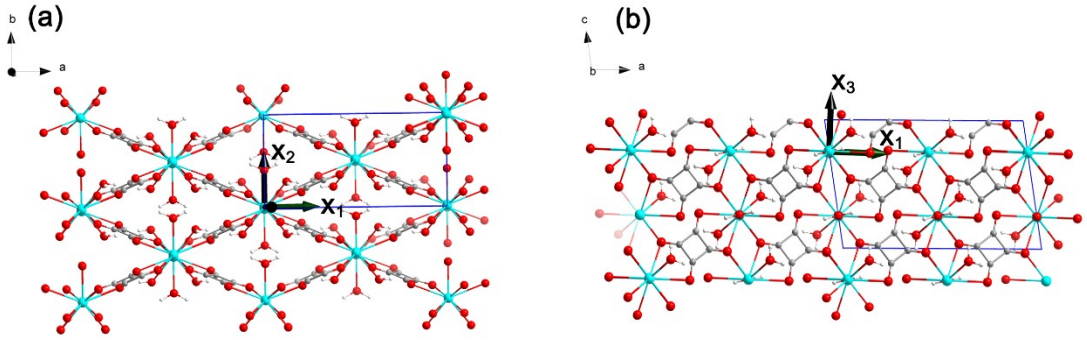

Figure S5 Illustration of the relationship between principal axes (blue lines) and orthorhombic axes (black arrows).

Table S1 Crystallographic data of compound **Sr-sq** at different temperatures**.**

Identification code	100 K	150 K	200 K	250 K	300 K
Empirical formula	$C_4H_6O_7Sr$	$C_4H_6O_7Sr$	$C_4H_6O_7Sr$	$C_4H_6O_7Sr$	$C_4H_6O_7Sr$
Formula weight	253.71	253.71	253.71	253.71	253.71
Temperature/K	100.09(10)	149.99(10)	199.96(10)	249.99(10)	299.94(10)
Crystal system	monoclinic	monoclinic	monoclinic	monoclinic	monoclinic
Space group	C2/c	C2/c	C2/c	C2/c	C2/c
a/Å	13.0755(7)	13.0683(7)	13.0650(7)	13.0653(7)	13.0565(8)
b/Å	6.4945(3)	6.5081(3)	6.5257(3)	6.5462(3)	6.5688(3)
c/Å	8.4711(5)	8.4763(4)	8.4886(4)	8.5027(4)	8.5163(5)
α/°	90	90	90	90	90
β/°	98.628(6)	98.566(5)	98.534(6)	98.518(6)	98.506(6)
γ/°	90	90	90	90	90
Volume/Å^3	711.22(7)	712.87(6)	715.71(6)	719.19(6)	722.37(7)
Z	4	4	4	4	4
ρ_{calc}g/cm^3	2.343	2.343	2.343	2.343	2.343
μ/mm^{-1}	7.580	7.496	7.496	7.496	7.496
F(000)	496.0	496.0	496.0	496.0	496.0
Crystal size/mm^3	0.1 × 0.1 × 0.1	0.1 × 0.1 × 0.1	0.1 × 0.1 × 0.1	0.1 × 0.1 × 0.1	0.1 × 0.1 × 0.1
Radiation	MoKα (λ = 0.71073)	MoKα (λ = 0.71073)	MoKα (λ = 0.71073)	MoKα (λ = 0.71073)	MoKα (λ = 0.71073)
2Θ range for data collection/°	8.27 to 59.28	8.26 to 59.368	8.246 to 59.326	8.226 to 59.262	8.742 to 59.222
Index ranges	-17 ≤ h ≤ 15, -8 ≤ k ≤ 8, -10 ≤ l ≤ 11	-17 ≤ h ≤ 17, -8 ≤ k ≤ 8, -10 ≤ l ≤ 11	-18 ≤ h ≤ 17, -8 ≤ k ≤ 8, -11 ≤ l ≤ 11	-17 ≤ h ≤ 18, -9 ≤ k ≤ 8, -11 ≤ l ≤ 11	-15 ≤ h ≤ 16, -9 ≤ k ≤ 8, -11 ≤ l ≤ 11
Reflections collected	3649	3444	3513	3470	3728
Independent reflections	896 [R_{int} = 0.0356, R_{sigma} = 0.0294]	899 [R_{int} = 0.0373, R_{sigma} = 0.0324]	911 [R_{int} = 0.0397, R_{sigma} = 0.0333]	902 [R_{int} = 0.0384, R_{sigma} = 0.0325]	901 [R_{int} = 0.0469, R_{sigma} = 0.0383]
Data/restraints/parameters	896/2/68	899/0/68	911/1/58	902/1/58	901/1/58
Goodness-of-fit on F^2	1.153	1.144	1.220	1.197	1.274
Final R indexes [I>=2σ (I)]	R_1 = 0.0263, wR_2 = 0.0654	R_1 = 0.0303, wR_2 = 0.0738	R_1 = 0.0379, wR_2 = 0.0939	R_1 = 0.0377, wR_2 = 0.0946	R_1 = 0.0391, wR_2 = 0.0972
Final R indexes [all data]	R_1 = 0.0272, wR_2 = 0.0658	R_1 = 0.0310, wR_2 = 0.0743	R_1 = 0.0391, wR_2 = 0.0947	R_1 = 0.0389, wR_2 = 0.0953	R_1 = 0.0404, wR_2 = 0.0979
Largest diff. peak/hole / e Å^{-3}	0.66/-1.37	0.48/-1.64	0.69/-2.04	0.81/-2.31	0.84/-2.28
CCDC number	2191456	2191453	2191454	2191452	2191455

Table S2 Distances of **Sr-sq** at different temperatures.

	100K	150K	200K	250K	300K
Sr-O1	2.540	2.544	2.541	2.545	2.548
Sr-O2	2.673	2.678	2.682	2.686	2.687
Sr-O3	2.534	2.535	2.535	2.536	2.539
Sr-O4	2.847	2.848	2.847	2.850	2.849
C1-C2	1.463	1.459	1.461	1.461	1.460
C1-O3	1.259	1.253	1.257	1.254	1.255
C2-O4	1.259	1.260	1.260	1.257	1.257
O1…O2	2.802	2.804	2.807	2.814	2.820

Table S3 Temperature dependent angle changes of φ_1 and φ_2

Temperature (K)	φ_1(˚)	φ_2(˚)
100	90.13(8)	127.17(1)
150	89.92(8)	127.05(1)
200	89.57(11)	126.92(1)
250	89.38(11)	126.78(1)
300	89.03(11)	126.59(1)

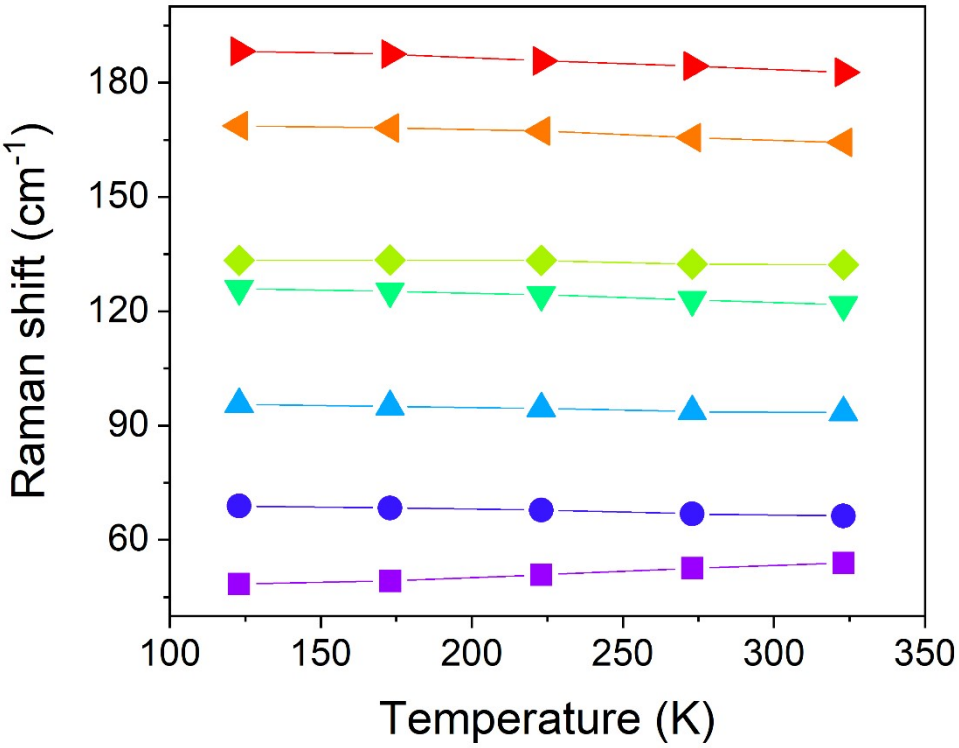

Figure S6 Temperature dependent low frequency (below 200 cm^{-1}) Raman mode shifts.

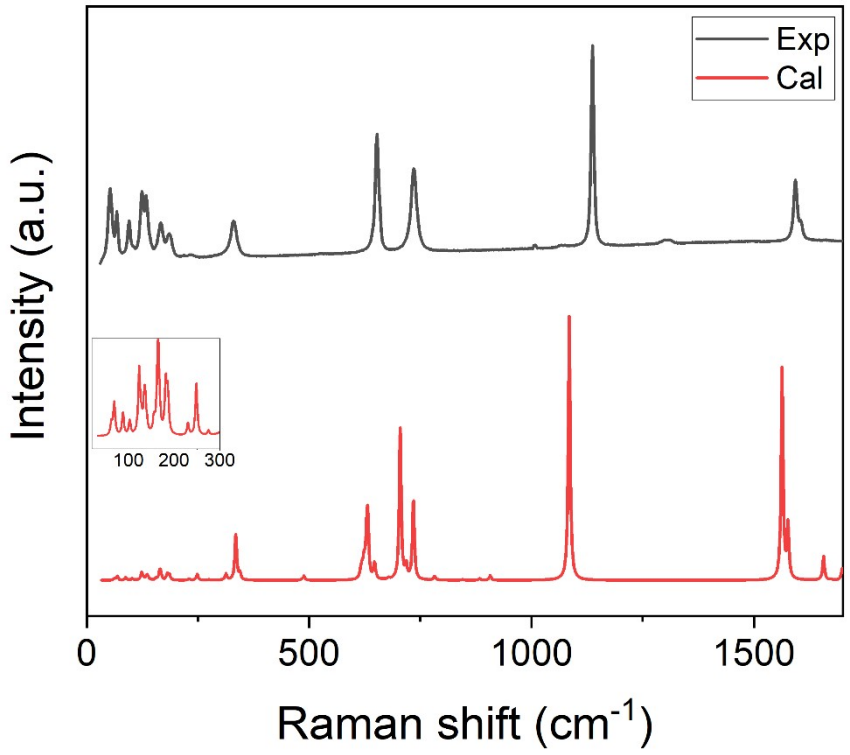

Figure S7 Experimental measured (black) and DFT calculated (red) Raman spectrum of **Sr-sq.**